

Received September 9, 2019, accepted September 30, 2019, date of publication October 4, 2019, date of current version October 17, 2019.

Digital Object Identifier 10.1109/ACCESS.2019.2945547

Maghemite Nanofluid Based on Natural Ester: Cooling and Insulation Properties Assessment

CRISTIAN OLMO¹, CRISTINA MÉNDEZ¹, FÉLIX ORTIZ¹, FERNANDO DELGADO¹,
RAFAEL VALIENTE², AND PETER WERLE³

¹Department of Electrical and Energy Engineering, ETSI Industriales y T., University of Cantabria, 39005 Santander, Spain

²Department of Applied Physics, Science Faculty, University of Cantabria, 39005 Santander, Spain

³Schering Institute, Leibniz Universität Hannover, 30167 Hannover, Germany

Corresponding author: Cristian Olmo (olmoc@unican.es)

This work was supported in part by the European Union's Horizon 2020 Research and Innovation Programme through the Marie Skłodowska-Curie under Grant 823969, and in part by the Ministry of Economy through the National Research Project: Improvement of Insulation Systems of Transformers through Dielectric Nanofluids under Grant DPI2015-71219-C2 1-R. The work of C. Olmo was supported by the University of Cantabria and the Government of Cantabria through Ph.D. Scholarship under Grant CVE-2016-6626.

ABSTRACT The objective of this work is to study the effect that the addition of magnetic nanoparticles to a natural ester has on its properties and its cooling capacity. Some samples of ferrofluid (natural ester with maghemite) have been prepared using different concentrations. These have been characterized by measuring their thermo-hydraulic and dielectric properties, to find an optimal concentration. Then, the cooling capacities of the optimal nanofluid and the base fluid have been tested in a transformer immersed in these liquids. The experimental platform allowed the measurement of temperatures in different locations at different load levels. Parallel simulations of these tests have been carried out with a Computational Fluid Dynamics model of the experimental platform. The results show an improvement of the insulating capacity of the base fluid with the addition of maghemite nanoparticles, and an enhanced cooling capacity.

INDEX TERMS CFD simulation, cooling, experimental platform, insulation, nanofluid, transformers.

I. INTRODUCTION

The electric grids will grow in importance in the mid-term due to the generalization of the electric transportation. The road transport represented more than the 25% of the final energy consumption in EU28 by 2015 [1], covered mainly by fossil fuels. Under the fight against pollution, the environmental public policies promote the transition of this demand towards renewable sources, intimately linked with the production of electricity, by increasing the share of electric vehicles. Thus, an increase of the percentage of energy delivered by the electric grid is expected.

Additionally, renewable energy sources (solar and wind power stations) can disrupt the planned operation of the Transmission System Operators (TSO) of the electric grid.

These challenges would be especially demanding for electric transformers, as nodes in networks. The grid resilience can be enhanced by the adoption of transformers with extra-loadability. These must be adapted to manage these levels of power in safety by increasing their efficiency. A traditional

problem is the weakness of the cellulosic insulation of transformer windings due to hot spots produced by high loads. As in other scientific fields, a possible solution could rise from the nanotechnology. The use of nanoparticles is growing in importance in medicine, in detection and treatments against cancer or in the administration of medicines [2], [3], in material science, obtaining enhanced properties polymers and materials for several applications [4], [5], in the treatment of industrial wastes, as they are able to capture polluting substances [6], and also in energy and thermal engineering, for energy and heat storage and cooling [7]–[9]. Beyond the advantages of the application of nanoparticles in technology, further considerations must be taken, regarding the consequences over the environment.

The improvement of transformer's cooling systems by the application of dielectric nanofluids is also under investigation since it was proposed in the late 90's [10]. This consist in the addition of a solid fraction of nanoparticles to traditional dielectric oils with the aim of improving their cooling capacities.

Several researches support this idea, mainly carried out by measuring how the thermal conductivity (k) of a mineral

The associate editor coordinating the review of this manuscript and approving it for publication was Giambattista Grusso¹.

transformer oil is affected by the presence of some metal oxide nanoparticles, by mean of the Hot Transient Wire technique (HTW). These nanoparticles have thermal conductivities several times higher than those usually found in dielectric oils, and with important differences between them [11]–[19].

Thus, Chiesa and Das [12], Choi *et al.* [20], and Xie *et al.* [21] developed Al_2O_3 oil-based nanofluids of different concentrations, between 0.25 and 1 vol.%, between 0.5 and 4 vol.%, and 5 vol.%, respectively. Their results reflect both an enhancement of the thermal conductivity of nanofluids respecting the base fluids, between 2 and 38%, and that these increases are bigger the higher the concentration of the solid fraction is. The resulting variation of the conductivity was equivalent among those concentrations similar enough. This is not the case with other nanoparticles whose k is lower, as they are SiO_2 , also investigated by Chiesa and Das [12], or TiO_2 , taken in consideration by Jin *et al.* [11] and Zhen Lv *et al.* [22]. In the first case, the same concentrations of nanoparticles produced an increase of conductivity around the half one obtained with Al_2O_3 . The second one has been used with concentrations around 0.1 vol.%, reaching variations of k up to 1.2%. On the contrary, iron species have shown better improvements of the thermal conductivity according to Nkurikiyimifura *et al.* [23], as concentrations between 1 and 5 vol.% reached enhancements of k in the range 10–60% in the absence of magnetic field.

This kind of studies has not only focused on thermal conductivity but also in other related properties. This is the case of the work developed by Mansour *et al.* [24], where the heat transfer coefficient (h) of Al_2O_3 nanofluids is tested. Here, with concentrations between 0.1 and 0.6 kg/m^3 , this research team found variations up to 15% respecting base fluid's h coefficient. This result points to a more pronounced effect of nanoparticles over h than over k , as with lower concentrations the enhancement of h was larger respecting those found over k in other studies. Peppas *et al.* [25] also studied the same parameter in nanofluids that combine Fe_2O_3 and vegetal base oil, with similar results, as the cooling was improved up to 45% with concentrations more than one hundred times less than those used by Nkurikiyimifura.

Nevertheless, other factors must be considered beyond the thermal properties, as oils play two different roles in transformers (cooling fluid and windings insulator). Several studies have demonstrated the additional positive effect of nanoparticles on dielectric properties such as breakdown voltage (BDV) of base fluids. However, in these studies, it has been found that there is a specific and low concentration that, if it is increased, this positive effect disappears. Hanai *et al.* [26] and Muangpratoom and Pattanadech [27] discovered that after improvements of BDV close to 25 % due to the presence of 0.05 and 0.03 vol.% of TiO_2 respectively, at higher concentrations this parameter started to decrease, with some results under the BDV of the base fluid, according to Hanai research. Peppas *et al.* [25], Irwanto *et al.* [28], Rafiq *et al.* [29], Imani *et al.* [30], and Primo *et al.* [31] found a similar situation with Fe_2O_3 and Fe_3O_4 nanofluids in

different concentrations (0.1 to 0.5 kg/m^3). Viscosity is another parameter that constraints the use of high concentrations [20].

As can be noticed in the mentioned researches, and in available reviews in this field, as those of Primo *et al.* [32], Ahmad *et al.* [33] or Patil *et al.* [34], most of the works in this field have focused on measurements of dielectric and thermal properties. Therefore, a closer approach to actual transformer oil operation conditions is needed.

In this sense, maghemite is one of the most promising nanoparticles, according to the references analyzed. This can be seen not only from the technical point of view. It has been demonstrated that nanoparticles are able to reach the environment from products which have them as components, as clothes, lotions or facade paints [35]. In these cases, depending on their size, concentration, shape, specific surface and composition, the nanoparticles can present a harmful effect on the living beings [35], [36]. They could affect the metabolism of the plants, the skin or the respiratory tract of the animals and they could even be stored in soft tissues and incorporated into the trophic chain [35], [36]. In [37], Arouja *et al.* shown that the toxicity of iron oxide nanoparticles could be classified as medium. Other different studies at higher concentrations support their limited effect [36], [38].

In parallel, several TSOs are starting to use transformers equipped with high-temperature insulating materials (natural esters and thermally upgraded Kraft papers) able to provide a permanent overloading up to 150% of nominal rating [39], [40].

This paper presents an experimental study on the impact of maghemite nanoparticles on the cooling capacity of a commercial natural ester. Before performing these tests, the characterization of fluid properties is conducted, to find the optimal concentration of maghemite according to nanofluids dielectric and/or thermal properties. Then, temperature variations in an experimental platform cooled by either a natural ester or maghemite nanofluid are compared at three load rates. The results obtained are compared with those from Computational Fluid Dynamics (CFD) models of the platform transformer. These simulations have proved previously to be reasonably accurate in the representation of the behaviour of nanofluids [41].

II. MATERIALS AND METHODS

A. EXPERIMENTAL TESTS

The properties of the base fluid, according to its manufacturer, are shown in Table 1. The solid fraction is composed of high purity maghemite spherical nanoparticles (CAS# 1309-37-1, Lot n°: FE-C1L20.1/091400500), with a mean size between 10 and 20 nm of diameter, according to the manufacturer (TECNAN).

The preparation of the samples follows the two-step method typically used in this kind of works. A certain amount of Fe_2O_3 nanoparticles is added carefully to the natural ester, and then the mixture is set under mechanic stirring for

TABLE 1. Main properties of vegetal base fluid.

| | |
|---|---------------------|
| Density (283K)(kg/m ³) | 910 |
| Kinematic viscosity (313K)(m ² /s) | <5·10 ⁻⁵ |
| Thermal conductivity (298K)(W/K·m) | 0.1691 |
| Dissipation factor (Tan δ) | <0.05 |
| AC Breakdown Voltage (V) | >35,000 |

15 minutes, followed by 12 hours under treatment with ultrasounds in a bath. With this procedure a proper distribution of the solid fraction is warranted.

Although during the preparation the samples are exposed to the environment, these are not submitted to any step of drying. They are just kept static for another 12 hours to dissipate any bubble arose during the process.

Although during the preparation the samples are exposed to the environment, these are not submitted to any step of drying. They are just kept static for another 12 hours to dissipate any bubble arose during the process.

The selected nanoparticle concentrations for the characterization of nanofluids properties are 0.1, 0.2, 0.3, 0.4 and 0.5 kg/m³, as this is the range where usually optimal concentrations, from the dielectric point of view, were noticed. Once the natural ester base fluid and the ferrofluids are prepared, the tests to measure their properties are carried out, following the methods set in the IEC standards, when available.

The thermal conductivity is measured at different temperatures using a KD2 Pro Thermal properties analyzer (5% uncertainty). Every 15 minutes the analyzer takes a thermal conductivity measurement while samples cool down from 323K to ambient temperature. To determine the viscosity and shear stress of samples a rotatory viscosimeter Haake viscotester 550 (0.5% uncertainty) is used. It needs 50 ml of sample for each test, measuring the dynamic viscosity at different temperatures, controlled by an external fluid circuit linked to a thermostatic bath. To analyze the shear stress both the base fluid and the highest-concentrated nanofluid have been subjected to controlled variations of the turning speed of the viscosimeter sensor. The rotor changes between three different and constant speed regimes, alternated with linear increasing and decreasing speed periods. Two series of these tests have been done for each sample, at ambient temperature. Regarding the density evolution with temperature, it is estimated with a density meter Mettler Toledo DM40 (0.1 kg/m³ measurement error), at six different temperatures between 293 and 343K.

Different dielectric properties are measured. The AC breakdown voltage is determined by a bA100 dielectric oil tester, using 400 ml of sample at rated temperature, according to IEC 60156 methodology. A BAUR DTL 2a is used to measure the resistivity and the loss factor. These tests are carried out with 45 ml of sample at 363K (IEC 60247). The moisture content is also controlled, since the dielectric

properties depend on this parameter, by Karl-Fischer Titration (IEC 60814) in a Metrohm 899 coulombmeter.

Following the experiment used by Patel *et al.* [42], an experimental setup was developed to study the cooling performance. The most promising ferrofluid among the studied ones has been tested in a prototype distribution transformer, in comparison with base oil (natural ester). This experimental platform has been made with a small single-phase transformer (800 VA, 115/230V), shown in Fig. 1 immersed in a tank, which acts as the casing of the machine. The two samples (about 6.5 liters each) are poured in the 20 cm × 20 cm × 20 cm casing, made of stainless steel, until the transformer is completely covered with coolant. This design was developed from the experience in previous works [43]. The sample movement inside the tank is driven only by natural convection cycles to dissipate the heat produced during operation. The platform temperatures are monitored by four probes located in strategic places of the transformer (top, bottom, iron and windings). The Fig. 1 shows, approximately, the location of the four probes. Also, an external probe was used to measure the ambient temperature, taken as reference. The measurement and recording of the temperatures are made by a microcontroller (Arduino) and an Integrated Development Environment (IDE).

The platform was tested in load tests with three different load levels, represented by load indexes C ($C = 0.7$, $C = 1$, $C = 1.3$). The rated currents of the transformer are 7A (115V) in the primary winding and 3.5A (230V) in the secondary winding. Each load index C is a coefficient for the rated current to be multiplied by, resulting the current at each load level. The load levels are reached by controlling three variable resistors, shown in the scheme of Fig. 1. In Table 2 the currents, voltages and resistances applied during the tests for each load index are summarized. With these values we assure the study of the behavior of the samples at different temperatures. The overload regime gives also temperatures closer to those found in actual distribution and power transformers.

The temperatures of the probes are caught every five seconds during the tests until the steady-state is reached and are available during the process. The stability criteria followed is the one defined in the IEC 60076-2, that establishes this condition is reached when the variation of the top oil's temperature rises below $1\text{K} \cdot \text{h}^{-1}$ over a consecutive period of 3 hours.

B. NUMERICAL TESTS

A numerical thermo-hydraulic 2D model of the experimental setup has been developed using Comsol Multiphysics 5.3a to study the fluid behavior in the experimental platform.

This study is based on the resolution on steady state of the governing equations that represent the physical phenomena during the work of the actual transformer. These are the equations of momentum and continuity of laminar regime, (1) and (2) respectively, and heat transfer (3), in the case of

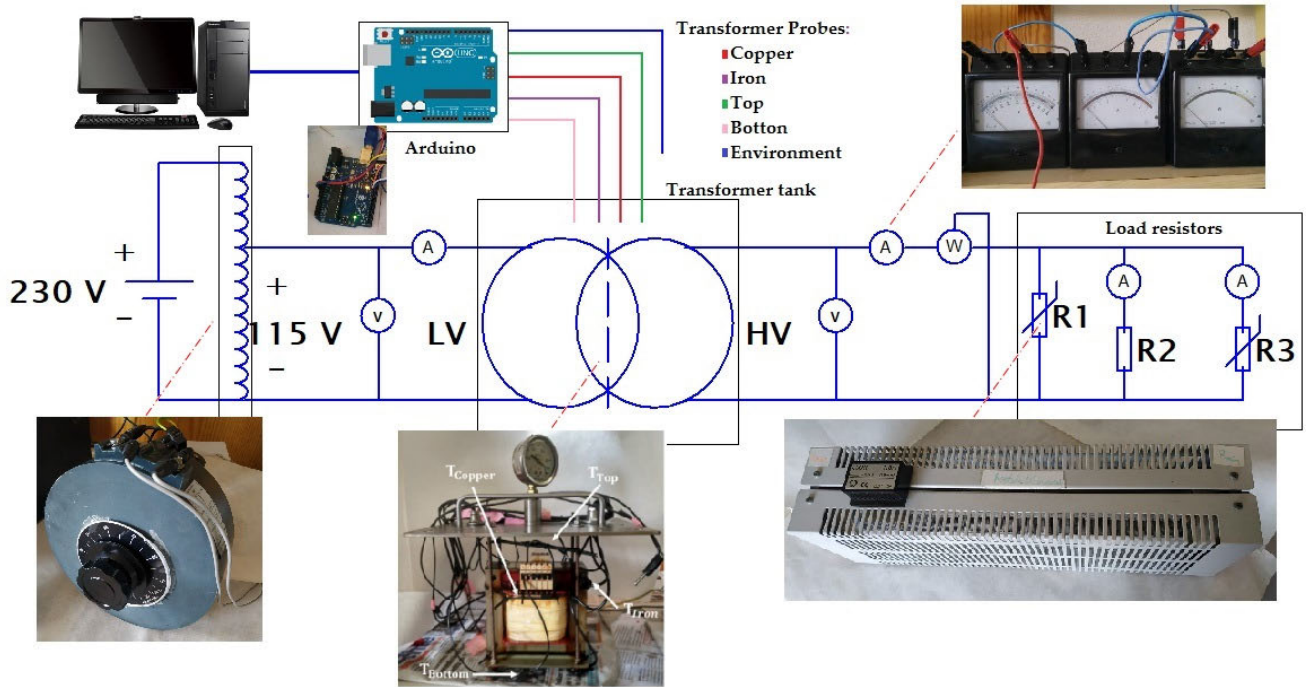


FIGURE 1. Connection scheme of the experimental platform.

TABLE 2. Circuit parameters in the load tests.

| Overload C=1.3; P=1040 W | |
|--------------------------|-----------------------|
| Primary winding | Secondary winding |
| $I_p=9\text{ A}$ | $I_s=4.5\text{ A}$ |
| $V_p=115\text{ V}$ | $V_s=230\text{ V}$ |
| | $Req.s=51.11\ \Omega$ |
| Rated power C=1; P=800 W | |
| Primary winding | Secondary winding |
| $I_p=6.96\text{ A}$ | $I_s=3.48\text{ A}$ |
| $V_p=115\text{ V}$ | $V_s=230\text{ V}$ |
| | $Req.s=65.71\ \Omega$ |
| Underload C=0.7; P=560 W | |
| Primary winding | Secondary winding |
| $I_p=4.87\text{ A}$ | $I_s=2.43\text{ A}$ |
| $V_p=115\text{ V}$ | $V_s=230\text{ V}$ |
| | $Req.s=94.46\ \Omega$ |

fluids, and the heat conduction equation (4) to define the heat flow in the solid parts:

$$P(u \cdot \nabla)u = -\nabla p + \nabla \cdot (\mu(\nabla u + (\nabla u)^T)) - 2/3\mu(\nabla \cdot u)I + g(\rho - \rho_{ref}) \quad (1)$$

$$\nabla \cdot (\rho u) = 0 \quad (2)$$

$$\rho \cdot C_p u \cdot \nabla T = \nabla \cdot (k \cdot \nabla T) + q_s \quad (3)$$

$$0 = -\nabla \cdot (k \cdot \nabla T) + q_s \quad (4)$$

In these equations ρ , u , P , μ , I , g , C_p , T and q_s are density, velocity vector, pressure, dynamic viscosity, identity matrix, standard gravity, specific heat capacity, temperature and heat source, respectively.

The 2D model is solved considering both the fluid and solid domains in the heat transfer. The coupling between heat transfer and laminar flow physics allows to calculate how the temperature changes affect the fluid properties related to the fluid flow.

The geometry of the model is defined by a section, shown in Fig. 2. The position of the experimental probes in the actual transformer is replicated in the model. A dense meshing of quadratic element in a direction perpendicular to the flow is used in the solid-liquid interface for a better capture of the velocity and temperature. Out of boundary layers, free triangular elements are used, as it can be noticed in Fig. 2.

The mathematical description of fluid properties regarding the temperature is based on the results from the fluid characterization, with the exception of the specific heat, whose mathematical expression was provided by the base fluid manufacturer. This last was also used to represent the nanofluids, in view of the scarce effect of the nanoparticles in the other properties at the concentrations used. Also, solid components of the experimental platform are considered. Their forming materials properties (density ρ , thermal conductivity k and specific heat C_p) are shown in Table 3, according to material distribution presented in Fig. 2. Comsol default libraries are the source of these data. Only k is taken into account by the heat transfer equation of the model (4), as it is solved in steady state.

As it was presented in [43], a simplifying process was necessary to model the experimental platform with a 2D section. Some simplifications and assumptions were considered to define the boundary conditions. Regarding heat transfer, axial

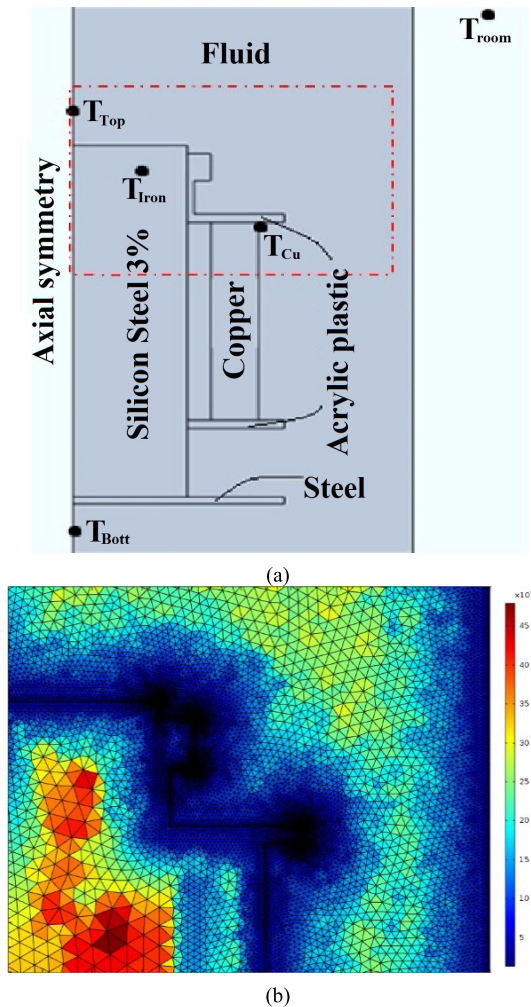


FIGURE 2. (a) 2D section of the modeled transformer; (b) detail of the meshing of the top right corner of the model.

TABLE 3. Model material properties at rated temperature, from Comsol data libraries.

| Material | ρ (kg/m ³) | k (W/(m K)) | C_p (J/(kg K)) |
|------------------|--------------------------------|------------------|---------------------|
| Silicon steel 3% | 7650 | 30.5 | 460 |
| Copper | 8960 | 400 | 385 |
| Acrylic plastic | 1190 | 0.18 | 1470 |
| Steel | 7850 | 44.5 | 475 |

symmetry is considered on the left edge. Also, negligible thermal resistance in the tank walls is applied to generate natural air convection. Finally, heat sources are uniform, both in the windings, due to Joule effect losses, and in the iron core, due to eddy currents and hysteresis, which were measured in experimental tests (short and open circuit tests respectively). The sum of these losses belongs to the heat source of the CFD model. Laminar flow also presents an axial symmetry in the left edge. No-slip condition is considered on the walls, so liquid velocity is zero in the wall-liquid interface. A pressure restriction point is set in the upper left corner. By last, buoyancy forces due to density differences in the fluid are considered as the origin of natural convection.

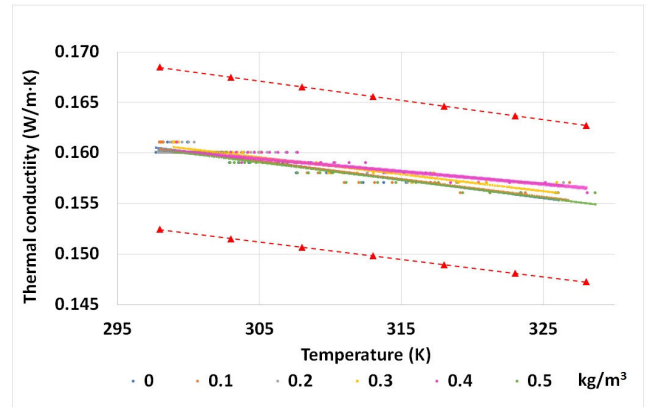


FIGURE 3. Evolution with temperature and nanoparticle concentration of thermal conductivity of samples.

The validation of the 2D numerical model is made by comparison between the temperatures obtained in the virtual probes and those measured by the probes in the experimental platform. A maximum difference of $\pm 1\%$ has been set as validation condition, with the temperatures expressed in K.

III. RESULTS

A. THERMAL AND DIELECTRIC CHARACTERIZATION OF FERROFLUIDS AND BASE OIL

The obtained results regarding the thermal conductivity of the tested samples are shown in Fig. 3, together with tendency lines and uncertainty gaps (red dashed lines). Here, no effect of nanoparticles can be noticed in thermal conductivity, as tendency lines almost meet each other and are inside tester error gap of $\pm 5\%$ respecting base fluid conductivity in the studied range of temperatures.

Again, very limited effect is found with dynamic viscosity, as it can be seen in Fig. 4, although in this case the variation of viscosity clearly overcomes the uncertainty gap (red dashed lines) in three of the nanoparticle concentrations. The same occurs with density, in Fig. 5, at each concentration. Their evolution with temperature is similar to those provided by manufacturers.

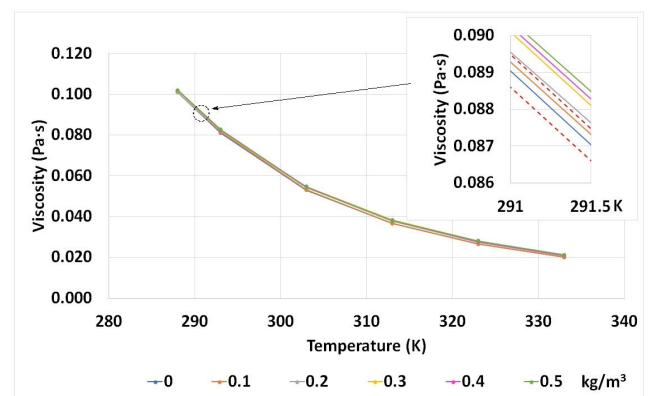


FIGURE 4. Evolution with temperature and nanoparticle concentration of dynamic viscosity of samples.

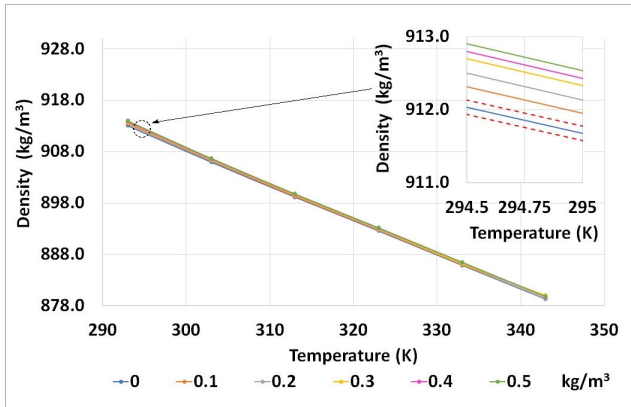


FIGURE 5. Evolution with temperature and nanoparticle concentration of density of samples.

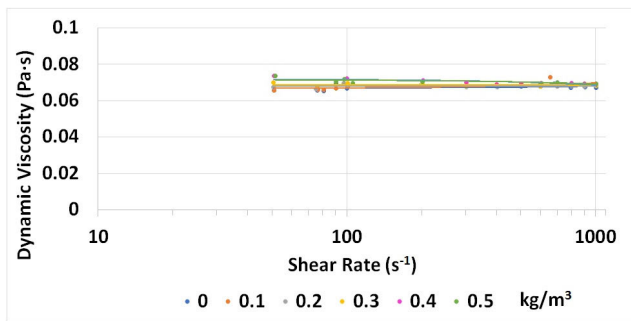


FIGURE 6. Viscosity vs shear stress for base fluid and most concentrated Fe_2O_3 nanofluid.

The analysis of the relationship between viscosity and shear stress seems to support the Newtonian behavior of the base fluid and the nanofluids. As can be seen in Fig. 6, the viscosity remains almost constant at different shear stress obtained from the rotor speed changes for tested samples. These viscosity values met with those previously showed at test temperature ($\approx 298K$). This absence of changes in viscosity at different shear stress is a characteristic of Newtonian fluids, as it means that they do not depend each other.

The distribution of values of breakdown voltage obtained in the tests is shown in Fig 7, together with the mean values for each concentration. Some of these values are lower than the one specified by the base fluid manufacturer for the dry natural oil due to the presence of moisture, whose mean levels are summarized in Fig 8. Water, as a polar substance, eases the transmission of charges in the oil, and reduces the voltage that the samples are capable to withstand [28].

As it can be seen in Fig. 7, the mean breakdown voltage of base fluid is slightly improved, especially at lower concentrations of nanoparticles, with a maximum enhancement of 16% at 0.2 kg/m^3 . At larger concentrations the effect is lost progressively, showing even voltages lower than the base fluid ones. It is also noticeable that these improvements occurred with samples with lightly larger contents of moisture regarding the base fluid, according to Fig. 8. With the same moisture contents, these improvements may have been even more pronounced. Another possible effect

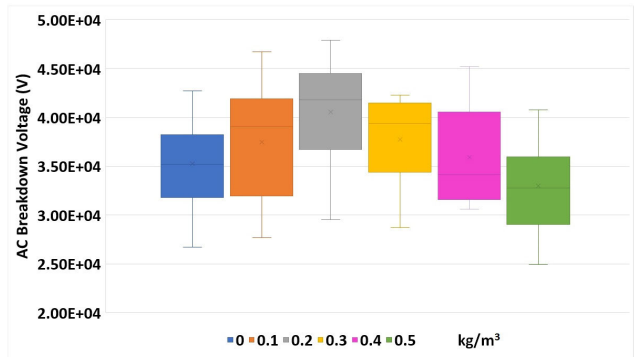


FIGURE 7. Dielectric strength results for each tested sample.

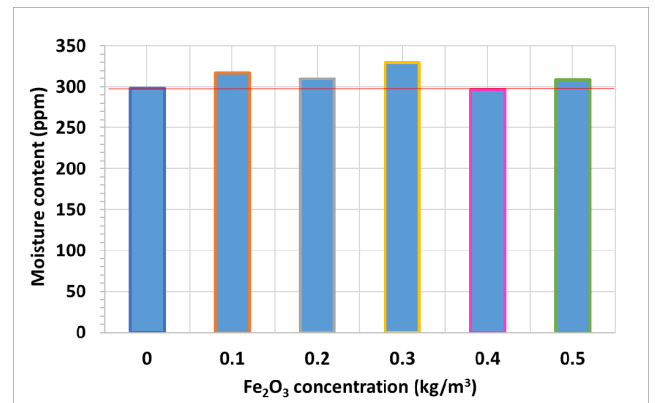


FIGURE 8. Mean moisture content of tested samples.

of moisture seems to appear regarding the extreme values of breakdown voltage distribution, as the sample with more moisture (0.3 kg/m^3) presents lower maximum and minimum values respecting close drier samples (0.2 and 0.4 kg/m^3). In these results, no interaction between the nanoparticles and the water molecules has been found.

Although the scarce effect of the tested concentrations on thermal properties, the increase of concentration trying to improve these properties is hindered by the evolution found in the breakdown voltage, as from 0.5 kg/m^3 this parameter is lower than that showed by the base fluid. The addition of nanoparticles must reach a compromise between dielectric and thermal properties variations.

Respecting the other dielectric parameters studied, according to Fig. 9, the dissipation factor ($\tan\delta$) experiences a continuous increase with the nanoparticles concentration raise, just the opposite tendency that is shown by both polarity resistivities (R). The values of the resistivity for each polarity differ each other less than the 35% set in the IEC 20247 for consecutive resistivity tests, so these results have been validated. This reverse effect of nanoparticles on these properties has already been noticed in other researches [31], [44].

In view of these results, following steps of the research were carried out with the optimum concentration found, in this case 0.2 kg/m^3 , according to its breakdown voltage. Due to the scarce effect of nanoparticles on them, thermal

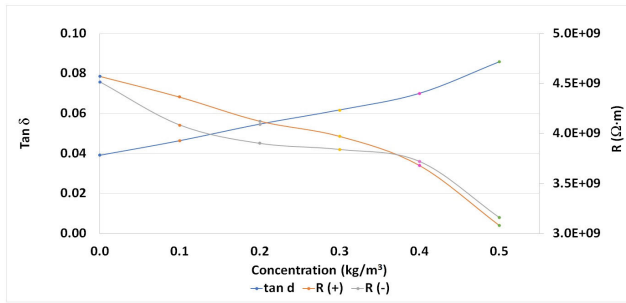


FIGURE 9. Dissipation factor and resistivity of tested samples.

TABLE 4. Temperature dependent equations for kinematic viscosity (ν), thermal conductivity (k), specific heat (C_p) and density (ρ) of fluids tested at the platform.

| | Base fluid | | 0.2 kg/m ³ Fe ₂ O ₃ Nanofluid | |
|-----------------------------|---|-----|--|------|
| ν (m ² /s) | $2.77981 \cdot e^{-0.0353523 \cdot T(K)}$ | (5) | $2.31182 \cdot e^{-0.034692 \cdot T(K)}$ | (9) |
| k (W/m·K) | $-1.84 \cdot 10^{-4} \cdot T(K) + 0.215312$ | (6) | $-1.22 \cdot 10^{-4} \cdot T(K) + 0.196548$ | (10) |
| C_p (J/K·kg) | $2.98 \cdot T(K) + 1088.1$ | (7) | $2.98 \cdot T(K) + 1088.1$ | (11) |
| ρ (kg/m ³) | $-0.674 \cdot T(K) + 1110.4$ | (8) | $-0.6809 \cdot T(K) + 1112.9$ | (12) |

properties cannot be considered. In order to be able to infer conclusions, the base fluid was also tested. For both fluids, the equations of their main properties according to the temperature were obtained from experimental results and the manufacturer (C_p). These are summarized in Table 4 and applied at the governing equations of the CFD model.

B. EXPERIMENTAL SETUP

The results obtained from the platform are shown in Table 5 as temperature gradients relative to the ambient temperature. In each probe, for both the natural ester base fluid and the ferrofluid, the temperature stability criteria were fulfilled. As it can be seen in this table, the increase of temperature is lower when ferrofluid is used as cooling fluid. The difference between the two fluids is higher in the overload regime (more heat to dissipate) and it decreases when the load rate is lower, up to almost zero for the underload regime in some of the probes. This is more noticeable by focusing on the gradients obtained at the windings, ΔT_{Cu} (Fig. 10). Here the differences noticed between the gradients for each cooling fluid and load index are expressed as a percentage reduction of temperature.

C. CFD SETUP SIMULATION

Considering the geometric simplifications applied and the small differences between the temperatures reached with both fluids in the experimental platform in $C = 1$ and $C = 0.7$ tests, it was decided to simulate the model only in the case of load index $C = 1.3$. As the temperature variations are more significant in this case, due to the larger load and heat dissipated, it may be more suitable to compare both the experimental and computational results for the ferrofluid and the base oil. In the other cases ($C = 1$ and $C = 0.7$) the differences are so small

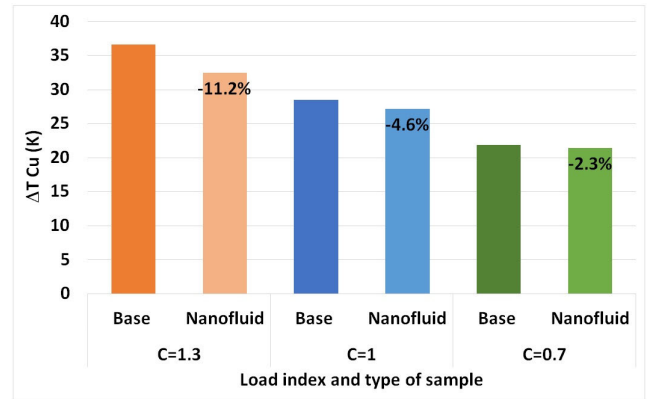


FIGURE 10. Thermal gradients in wire probes with different samples and loads.

TABLE 5. Experimental gradients of temperature (K) found per each fluid, load index C and probe.

| C | Fluid | ΔT_{Top} | ΔT_{Cu} | ΔT_{Iron} | ΔT_{Bottom} |
|-----|----------------------------------|------------------|-----------------|-------------------|---------------------|
| 1.3 | Base fluid | 32.7 | 36.6 | 36.6 | 25.6 |
| | 0.2 kg/m ³ Ferrofluid | 28.6 | 32.5 | 32.6 | 22.4 |
| 1 | Base fluid | 25.6 | 28.5 | 29.6 | 20.4 |
| | 0.2 kg/m ³ Ferrofluid | 23.9 | 27.2 | 28.1 | 20.1 |
| 0.7 | Base fluid | 19.9 | 21.9 | 24.4 | 16.8 |
| | 0.2 kg/m ³ Ferrofluid | 18.9 | 21.4 | 23.8 | 17.2 |

TABLE 6. Experimental and computational temperature test results at C = 1.3.

| Fluid | C=1.3 | Temperature (K) | | | | |
|---------------|--------------|-----------------|-------|-------|-------|--------|
| | | room | top | Cu | Fe | bottom |
| Natural Ester | Experimental | 301 | 333.7 | 337.6 | 337.6 | 326.6 |
| | Numerical | 301 | 334.8 | 338.5 | 338.3 | 328.4 |
| | % Deviation | 0 | 0.33 | 0.27 | 0.21 | 0.55 |
| Nanofluid | Experimental | 303 | 331.6 | 335.5 | 335.6 | 325.4 |
| | Numerical | 303 | 336.7 | 340.4 | 340.1 | 330.4 |
| | % Deviation | 0 | 1.54 | 1.46 | 1.34 | 1.54 |

that the experimental and numerical error considered prevent an adequate comparison.

Those results from the CFD simulations at overload regime are collected in Table 6, together with the experimental results to ease its comparison. Natural ester results reflect differences between experimental and computational temperatures (in K) lower than 1% in all the probes, so the CFD model has fulfilled the condition of validation. In the case of the nanofluid these differences are higher than 1%. In that case, the temperatures estimated by the numerical model are slightly higher than those obtained experimentally. This situation suggests that, in the ferrofluid, some additional forces or interactions appear, different from those that occur with the base fluid, not considered among the underlying physics of the CFD model.

IV. DISCUSSION AND CONCLUSION

The characterization and cooling testing of a Fe₂O₃ vegetal-based nanofluid for transformer application are presented

in this paper. The properties of both components and the preparation method of the samples are also described.

Six different concentrations (0 - 0.5 kg/m³) have been subjected to the measurement of different physical and dielectric properties as viscosity, thermal conductivity, density, dielectric strength, moisture content, resistivity and dissipation factor. Whereas no influence on the three first were noticed, probably due to the low concentrations of nanoparticles, an optimal improvement of natural ester AC Breakdown Voltage of 16% was found at 0.2 kg/m³ of Fe₂O₃. Similar conditions and results were found in two of the cited references, with iron nanoparticles [25], [29]. Resistivity and dissipation factor also show variations according to available bibliography. This dielectrically optimized nanofluid has been tested from the point of view of its cooling capacity in an experimental setup. A single-phase distribution transformer (800 VA) has been submerged in both samples of base fluid and nanofluid while working at three different load levels. Five temperature probes placed strategically in different points of the transformer have registered their temperature evolution. The results show a better behavior of the nanofluid respecting the base fluid, with lower gradients of temperature against the ambient one, up to -11.2 % at the largest load regime. This effect is less pronounced when the load of the transformer decreases. Thus, these nanofluids works better when the heat to dissipate is larger.

These experimental results have been checked against those obtained from a thermal-hydraulic CFD 2D model of the setup. While the model is validated when the transformer is cooled by the natural ester, this is not accurate enough to represent the behavior of the nanofluid.

Some conclusions can be drawn from the above. In the first place, the presence of nanoparticles enhances the breakdown voltage of natural ester, conditioned by the concentration of the nanofluid. The main theory that explains this is the supposed capacity of nanoparticles to capture and thus slow down the electrons, hindering the formation of discharges and streamers [19], [25], [29], [30]. This capacity might disappear at larger concentrations of nanoparticles as they build conductive bridges that ease the flow of electrons [25]. Its dependence on the presence of water molecules, widely certified in related literature [28], has also been noticed.

Other dielectric properties as dissipation factor or resistivity has suffered variations due to the presence of Fe₂O₃ nanoparticles, in function of their concentration. It seems that the presence of conductive particles supports conductivity processes, decreasing the resistivity. This, together with the polarization of the nanoparticles, supposes an increase of dielectric losses and thus of the dissipation factor [31], [44]. Logically, these variations are more pronounced at higher nanoparticles concentrations.

The Fe₂O₃ nanoparticles are also able to improve the cooling capacities of the base fluid. A reduction of hotspot winding temperature is found with the nanofluid as a coolant. This is especially significant as this parameter has a direct relation with the transformer' lifespan, that depends on the

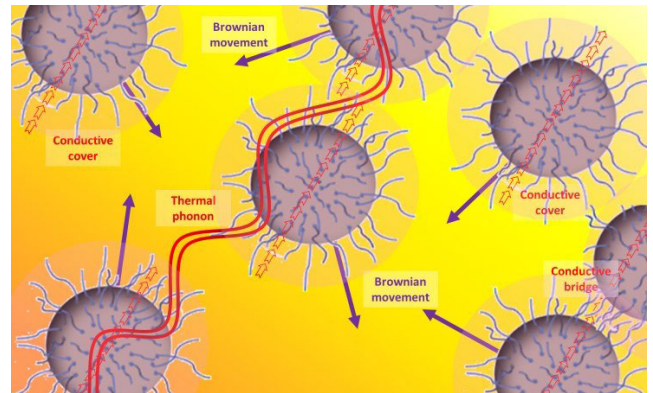


FIGURE 11. Heat transfer mechanisms in nanofluids.

structural integrity of dielectric cellulose in touch with the wires, susceptible to thermal degradation [45]. Although, this is not due to changes in viscosity or thermal conductivity with the addition of nanoparticles. The evolution of physical properties of base fluid does not show significant changes due to their presence, not enough by themselves to justify this effect. Improvements in thermal conductivity are usually explained according to four main theories, as they are the Brownian motion of the nanoparticles in the fluid, conductive covers due to the ordering of fluid molecules around the particle, conductive bridges due to particle aggregation or the transmission of heat in ballistic thermal phonons [18], [46], [47], shown in Fig. 11. In this case they are not suitable to explain the improvement in convection, as no changes have been noticed in conductivity. The appearance of these phenomena may be constrained by low nanoparticle concentrations, and the addition of larger concentrations is hindered by the evolution of dielectric properties.

In parallel to this, the disability of the validated CFD model to represent the behavior of the nanofluid triggers the idea of the presence in the tested nanofluid samples of other forces beyond those considered during the simulations. An explanation for the improved cooling capacity of ferrofluids is the interaction between the ferrofluid and the magnetic field generated by the transformer, since this interaction was not considered by the CFD model. This has been noticed and explained in other works: the existence of thermomagnetic convection due to the changes in magnetic susceptibility between the hotter and colder parts of the ferrofluid [42], [48]. This difference raises when the amount of heat to dissipate increases, as the magnetic susceptibility decreases with the temperature. Further research with non-magnetic nanoparticles in similar conditions is necessary from this point, to check their effect on the cooling of the experimental setup.

The applicability of these nanofluids would depend on many aspects. Firstly, from the environmental standpoint, the application of ferrofluids in transformers would not suppose potential danger. According to the consulted references, these nanoparticles have a limited effect at the concentrations proposed. Also, it should be considered the location of the

transformers in pits, designed to minimize pollution from the scarce dielectric oil leakages to the environment.

Secondly, the results show an improvement of the effect of the nanoparticles with the temperature: the closer are the working temperatures to those of the real distribution and power transformers, the higher is the improvement.

Finally, it would be necessary to study other aspects of the application of nanofluids in transformers, as the evolution of their properties in working conditions, their performance in complex forced cooling circuits or how they would affect equipment as pipes or pumps.

If their viability is confirmed, the effect of nanoparticles on cooling and dielectric capacities, in case of application of this nanofluid in the cooling circuits of transformers, would allow transformers to work at higher loads or in safer conditions dealing with the challenges to come.

REFERENCES

- [1] *Energy, Transport and Environment Indicators 2017 Edition*, Eurostat, Brussels, Belgium, 2017.
- [2] J. D. Courtois, I. Bazán, A. Vera, and L. Leija, "Temperature increase in magnetic nanoparticles by magnetic field induction for hyperthermia treatment," in *Proc. Global Med. Eng. Phys. Exchanges Pan Amer. Health Care Exchanges*, 2019, pp. 1–6.
- [3] M. Gökçe, A. Alemdar, and S. Işçi, "Comparison of ionic polymers in the targeted drug delivery applications as the coating materials on the Fe₃O₄ nanoparticles," *Mater. Sci. Eng., C*, vol. 103, Oct. 2019, Art. no. 109838.
- [4] I. M. Nikbin, R. Mohebbi, S. Dezhmanpanah, S. Mehdipour, R. Mohammadi, and T. Nejat, "Gamma ray shielding properties of heavy-weight concrete containing nano-TiO₂," *Radiat. Phys. Chem.*, vol. 162, pp. 157–167, Sep. 2019.
- [5] N. Mamidi, M. Renato, M. Gamero, J. Villela, and A. Elfas, "Development of ultra-high molecular weight polyethylene-functionalized carbon nanofibers composites for biomedical applications," *Diamond Rel. Mater.*, vol. 97, Aug. 2019, Art. no. 107435.
- [6] S. M. Pourmortazavi, H. Sahebi, H. Zandavar, and S. Mirsadeghi, "Fabrication of Fe₃O₄ nanoparticles coated by extracted shrimp peels chitosan as sustainable adsorbents for removal of chromium contaminates from wastewater: The design of experiment," *Compos. B, Eng.*, vol. 175, Oct. 2019, Art. no. 107130.
- [7] L. Wang, N. Liu, and Y. Zhao, "Nanoporous TiO₂/MoO₃/Fe₃O₄ composite as anode for high-performance lithium-ion batteries," *Solid State Sci.*, vol. 95, Sep. 2019, Art. no. 105930.
- [8] M. Sheikholeslami, R.-U. Haq, A. Shafee, Z. Li, Y. G. Elaraki, and I. Tlili, "Heat transfer simulation of heat storage unit with nanoparticles and fins through a heat exchanger," *Int. J. Heat Mass Transf.*, vol. 135, pp. 470–478, Jun. 2019.
- [9] L. K. Kadirgama, K. Anamalai, K. Ramachandran, D. Ramasamy, M. Samykano, A. Kottasamy, and M. M. Rahman, "Thermal analysis of SUS 304 stainless steel using ethylene glycol/nanocellulose-based nanofluid coolant," *Int. J. Adv. Manuf. Technol.*, vol. 97, nos. 5–8, pp. 2061–2076, Jul. 2018.
- [10] V. Segal, A. Hjortsberg, A. Rabinovich, D. Natrass, and K. Raj, "AC (60 Hz) and impulse breakdown strength of a colloidal fluid based on transformer oil and magnetite nanoparticles," in *Proc. IEEE Int. Symp. Elect. Insul.*, vol. 2, Jun. 1998, pp. 619–622.
- [11] H. Jin, T. Andritsch, I. A. Tsekmes, R. Kochetov, P. H. F. Morshuis, and J. J. Smit, "Thermal conductivity of fullerene and TiO₂ nanofluids," in *Proc. Annu. Rep. Conf. Elect. Insul. Dielectric Phenomena*, Oct. 2013, pp. 711–714.
- [12] M. Chiesa and S. K. Das, "Experimental investigation of the dielectric and cooling performance of colloidal suspensions in insulating media," *Colloids Surf. A Physicochem. Eng. Aspects*, vol. 335, nos. 1–3, pp. 88–97, 2009.
- [13] J. Taha-Tijerina, T. N. Narayanan, G. Gao, M. Rohde, D. A. Tsentlovich, M. Pasquali, and P. M. Ajayan, "Electrically insulating thermal nano-oils using 2D fillers," *ACS Nano*, vol. 6, no. 2, pp. 1214–1220, Jan. 2012.
- [14] W. Yu and H. Xie, "A review on nanofluids: Preparation, stability mechanisms, and applications," *J. Nanomater.*, vol. 2012, Jul. 2012, Art. no. 435873.
- [15] M. Rajnak, M. Timko, P. Kopcansky, K. Paulovicova, J. Tothova, J. Kurimsky, B. Dolnik, R. Cimbala, M. V. Avdeev, V. I. Petrenko, and A. Feoktystov, "Structure and viscosity of a transformer oil-based ferrofluid under an external electric field," *J. Magn. Magn. Mater.*, vol. 431, pp. 99–102, Jun. 2017.
- [16] M.-S. Liu, M. C.-C. Lin, I.-T. Huang, and C.-C. Wang, "Enhancement of thermal conductivity with CuO for nanofluids," *Chem. Eng. Technol.*, vol. 29, no. 1, pp. 72–77, Jan. 2006.
- [17] F. D. Stoian, S. Holotescu, A. Taculescu, O. Marinica, D. Resiga, M. Timko, P. Kopcansky, and M. Rajnak, "Characteristic properties of a magnetic nanofluid used as cooling and insulating medium in a power transformer," in *Proc. 8th Int. Symp. Adv. Topics Elect. Eng. (ATEE)*, May 2013, pp. 23–26.
- [18] S. A. Angayarkanni and J. Philip, "Review on thermal properties of nanofluids: Recent developments," *Adv. Colloid Interface Sci.*, vol. 225, pp. 146–176, Nov. 2015.
- [19] J. G. Hwang, M. Zahn, F. M. O'Sullivan, L. A. A. Pettersson, O. Hjortstam, and R. Liu, "Effects of nanoparticle charging on streamer development in transformer oil-based nanofluids," *J. Appl. Phys.*, vol. 107, Oct. 2010, Art. no. 014310.
- [20] C. Choi, H. S. Yoo, and J. M. Oh, "Preparation and heat transfer properties of nanoparticle-in-transformer oil dispersions as advanced energy-efficient coolants," *Current Appl. Phys.*, vol. 8, no. 6, pp. 710–712, 2008.
- [21] H. Xie, J. Wang, T. Xi, Y. Liu, and F. Ai, "Dependence of the thermal conductivity of nanoparticle-fluid mixture on the base fluid," *J. Mater. Sci. Lett.*, vol. 21, no. 19, pp. 1469–1471, Oct. 2002.
- [22] Y.-Z. Lv, C. Li, Q. Sun, M. Huang, C.-R. Li, and B. Qi, "Effect of dispersion method on stability and dielectric strength of transformer oil-based TiO₂ nanofluids," *Nanosci. Res. Lett.*, vol. 11, no. 1, pp. 4–9, Dec. 2016.
- [23] I. Nkurikiyimfura, Y. Wang, and Z. Pan, "Effect of chain-like magnetite nanoparticle aggregates on thermal conductivity of magnetic nanofluid in magnetic field," *Exp. Therm. Fluid Sci.*, vol. 44, pp. 607–612, Jan. 2013.
- [24] D.-E. A. Mansour and A. M. Elsaed, "Heat transfer properties of transformer oil-based nanofluids filled with Al₂O₃ nanoparticles," in *Proc. IEEE Int. Conf. Power Energy (PECon)*, Dec. 2014, pp. 123–127.
- [25] G. D. Peppas, "Ultrastable natural ester-based nano fluids for high voltage insulation applications," *ACS Appl. Mater. Interfaces*, vol. 8, no. 38, pp. 25202–25209, Sep. 2016.
- [26] M. Hanai, S. Hosomi, H. Kojima, N. Hayakawa, and H. Okubo, "Dependence of TiO₂ and ZnO nanoparticle concentration on electrical insulation characteristics of insulating oil," in *Proc. Annu. Rep. Conf. Elect. Insul. Dielectric Phenomena (CEIDP)*, Oct. 2013, pp. 780–783.
- [27] P. Muangpratoom and N. Pattanadach, "Breakdown and partial discharge characteristics of mineral oil-based nanofluids," *IET Sci., Meas. Technol.*, vol. 15, no. 5, pp. 609–616, Aug. 2018.
- [28] Irwanto, C. G. Azcarraga, Suwarno, A. Cavallini, and F. Negri, "Ferrofluid effect in mineral oil: PDIV, streamer, and breakdown voltage," in *Proc. Int. Conf. High Voltage Eng. Appl. (ICHVE)*, Sep. 2014, pp. 3–6.
- [29] M. Rafiq, C. Li, Y. Ge, Y. Lv, and K. Yi, "Effect of Fe₃O₄ nanoparticle concentrations on dielectric property of transformer oil," in *Proc. IEEE Int. Conf. High Voltage Eng. Appl. (ICHVE)*, Sep. 2016, pp. 1–4.
- [30] M. T. Imani, J. F. Miethe, P. Werle, N. C. Bigall, and H. Borsi, "Engineering of multifunctional nanofluids for insulation systems of high voltage apparatus," in *Proc. IEEE Conf. Elect. Insul. Dielectric Phenomena (CEIDP)*, Oct. 2016, pp. 44–47.
- [31] V. A. Primo, D. Pérez-Rosa, B. García, and J. C. Cabanelas, "Evaluation of the stability of dielectric nanofluids for use in transformers under real operating conditions," *Nanomaterials*, vol. 9, no. 2, p. 143, Feb. 2019.
- [32] V. A. Primo, B. Garcia, and R. Albarracin, "Improvement of transformer liquid insulation using nanodielectric fluids: A review," *IEEE Elect. Insul. Mag.*, vol. 34, no. 3, pp. 13–26, May/Jun. 2018.
- [33] F. Ahmad, A. A. Khan, Q. Khan, and M. R. Hussain, "State-of-art in nano-based dielectric oil: A review," *IEEE Access*, vol. 7, pp. 13396–13410, 2019.
- [34] M. S. Patil, J. H. Seo, S. J. Kang, and M. Y. Lee, "Review on synthesis, thermo-physical property, and heat transfer mechanism of nanofluids," *Energies*, vol. 9, no. 10, p. 840, 2016.

- [35] T. Vlachogianni and A. Valavanidis, "Nanomaterials: Environmental pollution, ecological risks and adverse health effects," *Nano Sci. Nano Technol.*, vol. 8, no. 6, pp. 208–226, 2014.
- [36] J. López-Luna, M. M. Camacho-Martínez, F. A. Solís-Domínguez, M. C. González-Chávez, R. Carrillo-González, S. Martínez-Vargas, O. F. Mijangos-Ricardez, and M. C. Cuevas-Díaz, "Toxicity assessment of cobalt ferrite nanoparticles on wheat plants," *J. Toxicol. Environ. Health*, vol. 81, no. 14, pp. 604–619, Jul. 2018.
- [37] V. Aruoja, S. Pokhrel, M. Sihtmäe, M. Mortimer, L. Mädler, and A. Kahru, "Toxicity of 12 metal-based nanoparticles to algae, bacteria and protozoa," *Environ. Sci. Nano*, vol. 2, no. 6, pp. 630–644, 2015.
- [38] Z. Xia, G. Wang, K. Tao, J. Li, and Y. Tian, "Preparation and acute toxicology of nano-magnetic ferrofluid," *J. Huazhong Univ. Sci. Technol.*, vol. 25, no. 1, pp. 59–61, Feb. 2005.
- [39] F. Scatiggio, C. Serafino, and F. Pepe, "Increased loadability of transformers immersed in natural ester," in *Proc. IEEE 20th Int. Conf. Dielectric Liquids (ICDL)*, Jun. 2019, pp. 1–4.
- [40] V. Vasconcellos, A. Sbravati, L. C. Zanetta, K. Rapp, L. Lombini, S. Nazzari, F. Scatiggio, and A. Valant, "Increased loadability of transformers using natural ester and cellulosic materials as high temperature insulation systems," *IEEE Elect. Insul. Mag.*, vol. 34, no. 5, pp. 8–17, Sep. 2018.
- [41] O. Mahian, L. Kolsi, M. Amani, P. Estellé, G. Ahmadi, C. Kleinstreuer, J. S. Marshall, R. A. Taylor, E. Abu-Nada, S. Rashidi, H. Niazmand, S. Wongwises, T. Hayat, A. Kasaiean, and L. Pop, "Recent advances in modeling and simulation of nanofluid flows—Part II: Applications," *Phys. Rep.*, vol. 791, pp. 1–59, Feb. 2019.
- [42] J. Patel, K. Parekh, and R. V. Upadhyay, "Prevention of hot spot temperature in a distribution transformer using magnetic fluid as a coolant," *Int. J. Therm. Sci.*, vol. 103, pp. 35–40, May 2016.
- [43] A. Ortiz, F. Delgado, F. Ortiz, I. Fernández, and A. Santisteban, "The aging impact on the cooling capacity of a natural ester used in power transformers," *Appl. Therm. Eng.*, vol. 144, pp. 797–803, Nov. 2018.
- [44] R. Liu, L. A. A. Pettersson, T. Auletta, and O. Hjortstam, "Fundamental research on the application of nano dielectrics to transformers," in *Proc. Annu. Rep. Conf. Elect. Insul. Dielectric Phenomena*, Oct. 2011, pp. 423–427.
- [45] F. Delgado, A. Ortiz, I. Fernandez, A. Arroyo, and J. A. Macías, "Study on the cooling capacity of alternative liquids in power transformers," in *Proc. Elect. Syst. Aircr., Railway Ship Propuls.*, Oct. 2012, pp. 1–6.
- [46] P. Koblinski, S. R. Phillpot, S. U. S. Choi, and J. A. Eastman, "Mechanisms of heat flow in suspensions of nano-sized particles (nanofluids)," *Int. J. Heat Mass Transf.*, vol. 45, no. 4, pp. 855–863, Apr. 2001.
- [47] L. T. Benos, E. G. Karvelas, and I. E. Sarris, "A theoretical model for the magnetohydrodynamic natural convection of a CNT-water nanofluid incorporating a renovated Hamilton-Crosser model," *Int. J. Heat Mass Transf.*, vol. 135, pp. 548–560, Jun. 2019.
- [48] L. Pislaru-Danescu, A. M. Morega, M. Morega, V. Stoica, O. M. Marinică, F. Nourag, N. Păduraru, I. Borbáth, and T. Borbáth, "Prototyping a ferrofluid-cooled transformer," *IEEE Trans. Ind. Appl.*, vol. 49, no. 3, pp. 1289–1298, May/Jun. 2013.



CRISTINA MÉNDEZ was born in Santander, Spain, in 1996. She received the M.Sc. degree from the Industrial Engineering Research, University of Cantabria, in 2019, where she is currently a Researcher of the Electrical and Energy Engineering Department. Her main research interest includes currently the study of dielectric nanofluids.



FÉLIX ORTIZ received the M.Sc. degree in physical sciences, in 2000, and the Ph.D. degree from the University of Cantabria (UC), Spain, in 2016, where he is currently an Aggregate Professor with the Electrical and Energy Engineering Department. He has presented more than ten articles at international conferences and has published four journal articles. His main research interest includes alternative dielectric liquids for power transformers.



FERNANDO DELGADO was born in Santander, in 1968. He received the M.Sc. degree in industrial engineering, in 1998, and the Ph.D. degree from the University of Cantabria (UC), Spain, in 2011, where he is currently an Associate Professor with the Electrical and Energy Engineering Department. He has published over 25 works in international conferences and 13 articles in journals included in the Journal of Citation Report. His main research interest includes currently the study of the alternative dielectric liquids in power transformers.



RAFAEL VALIENTE received the B.Sc. degree in physics from the University of Cantabria, in 1991, and the Ph.D. degree in physics, in 1998, where he is currently an Associate Professor of physics with the Applied Physics Department. He has contributed to more than 120 reviewed journal articles and more than 40 international conferences. His main research interests include the design, synthesis, and characterization of materials and nanomaterials.



PETER WERLE is currently a Professor with the High voltage technology and Asset management Department, Leibniz Universität Hannover. He is also the Head of Scheging-Institute (Institute of electrical energy systems). He has published more than ten articles in journals and several international conferences. His main research interest includes the study of high voltage technology and monitoring of high voltage systems.



CRISTIAN OLMO was born in Santander, Spain, in 1983. He received the M.Sc. degree in mining engineering from the University of Cantabria, Spain, in 2016, where he is currently pursuing the Ph.D. degree. Finally, his main research interest includes currently the study of the dielectric nanofluids.